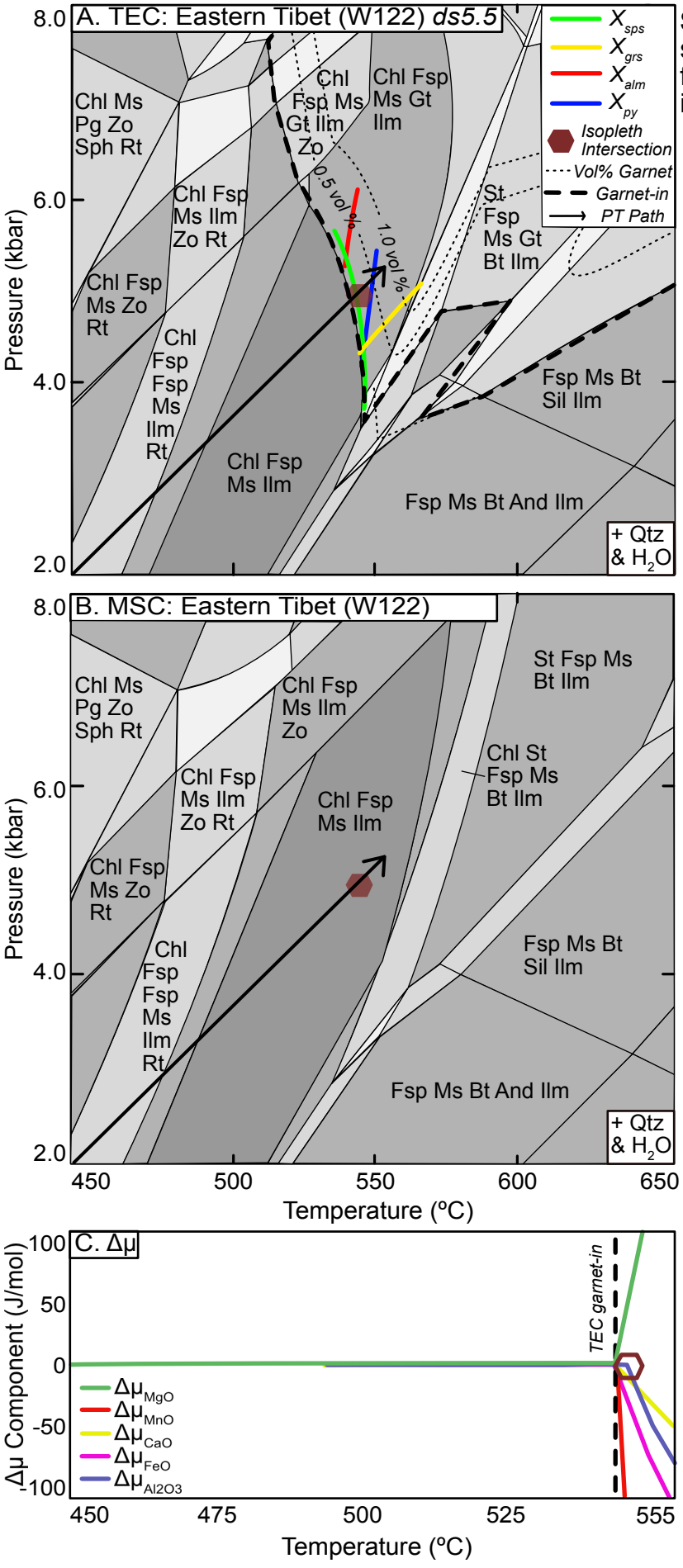

Supplemental Figure 1: A. TEC pseudosection for sample W122 (Eastern Tibet). B. MSC pseudosection for sample W122. C. $\Delta\mu_{component}$ along *P-T* path shown in A & B.

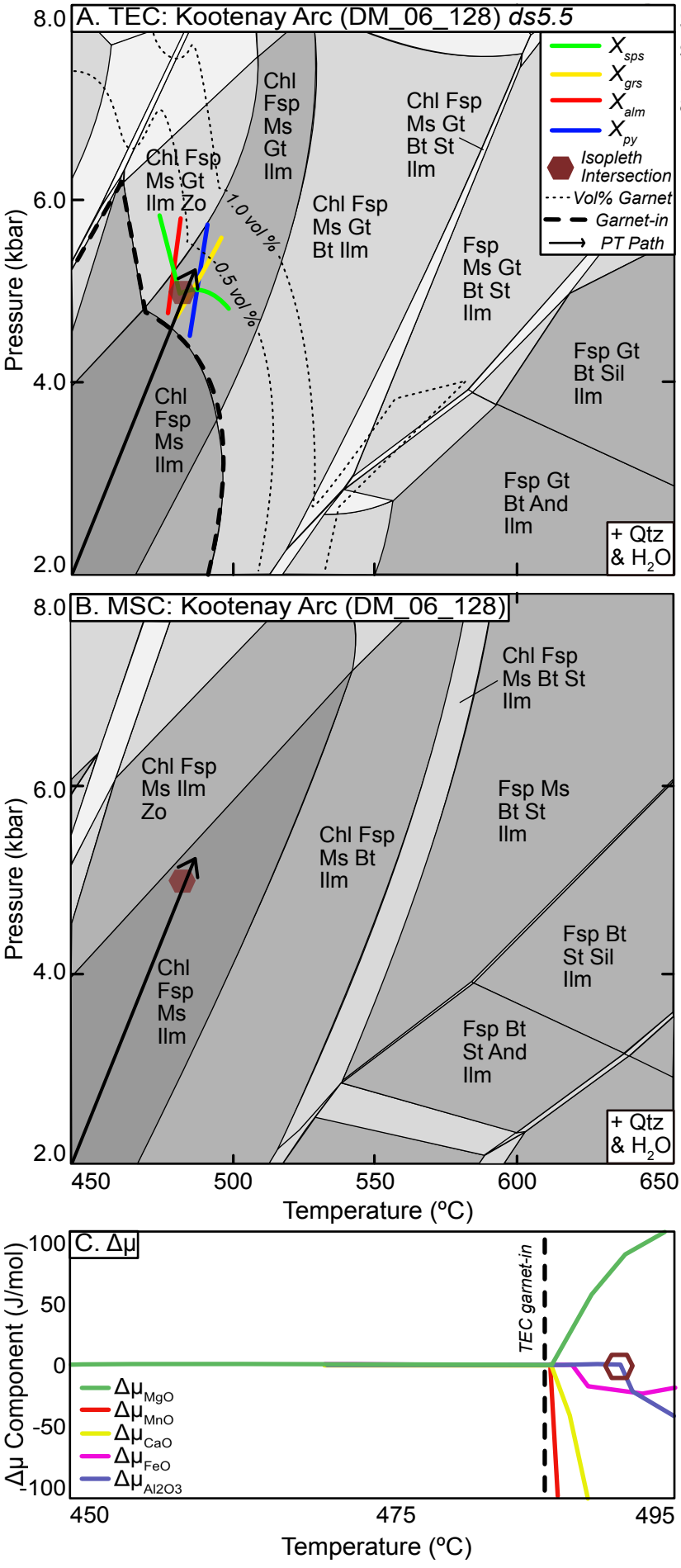

Supplemental Figure 2: A. TEC pseudosection for sample DM_06_128 (Kootenay Arc). B. MSC pseudosection for sample DM_06_128. C. $\Delta\mu_{component}$ along *P-T* path shown in A & B.

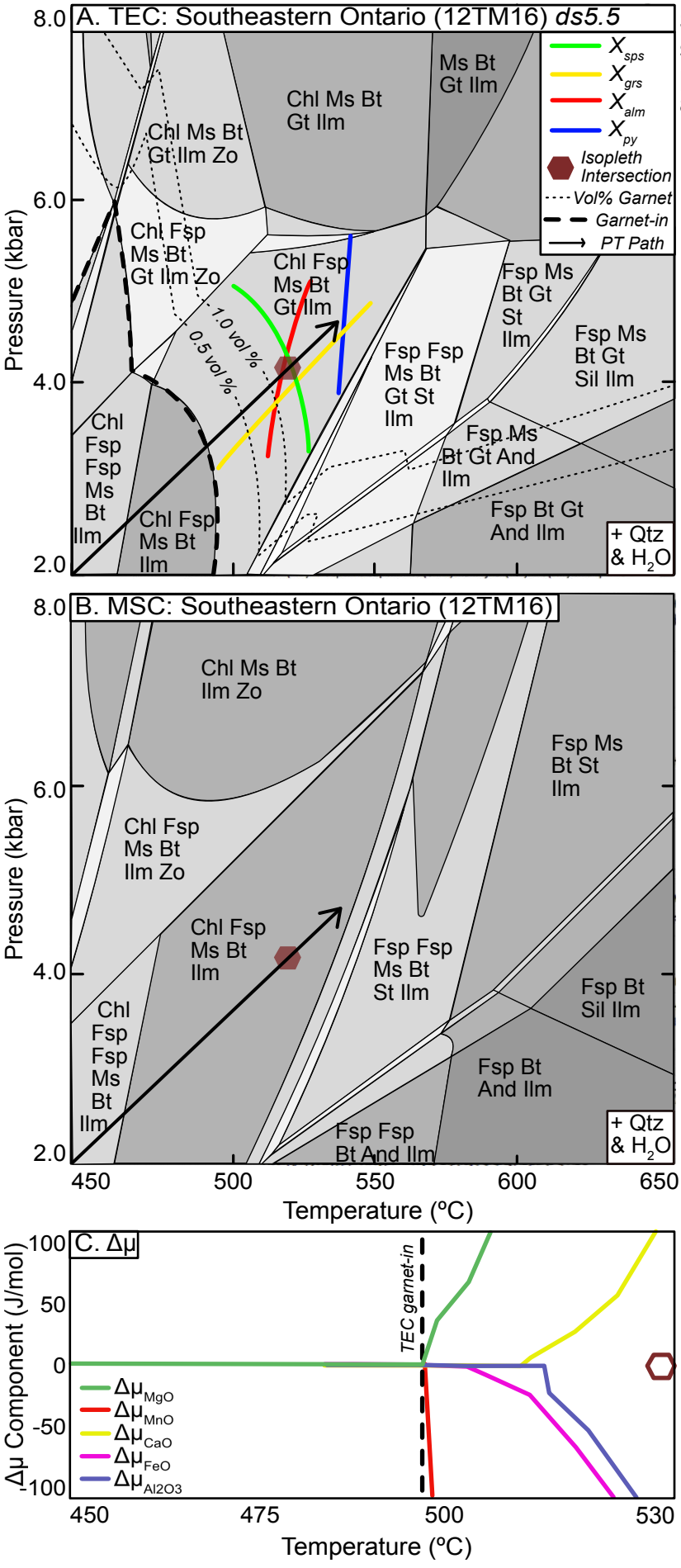

Supplemental Figure 3: A. TEC pseudosection for sample 12TM16 (Southeastern Ontario). B. MSC pseudosection for sample 12TM16. C. $\Delta\mu_{component}$ along *P-T* path shown in A & B.

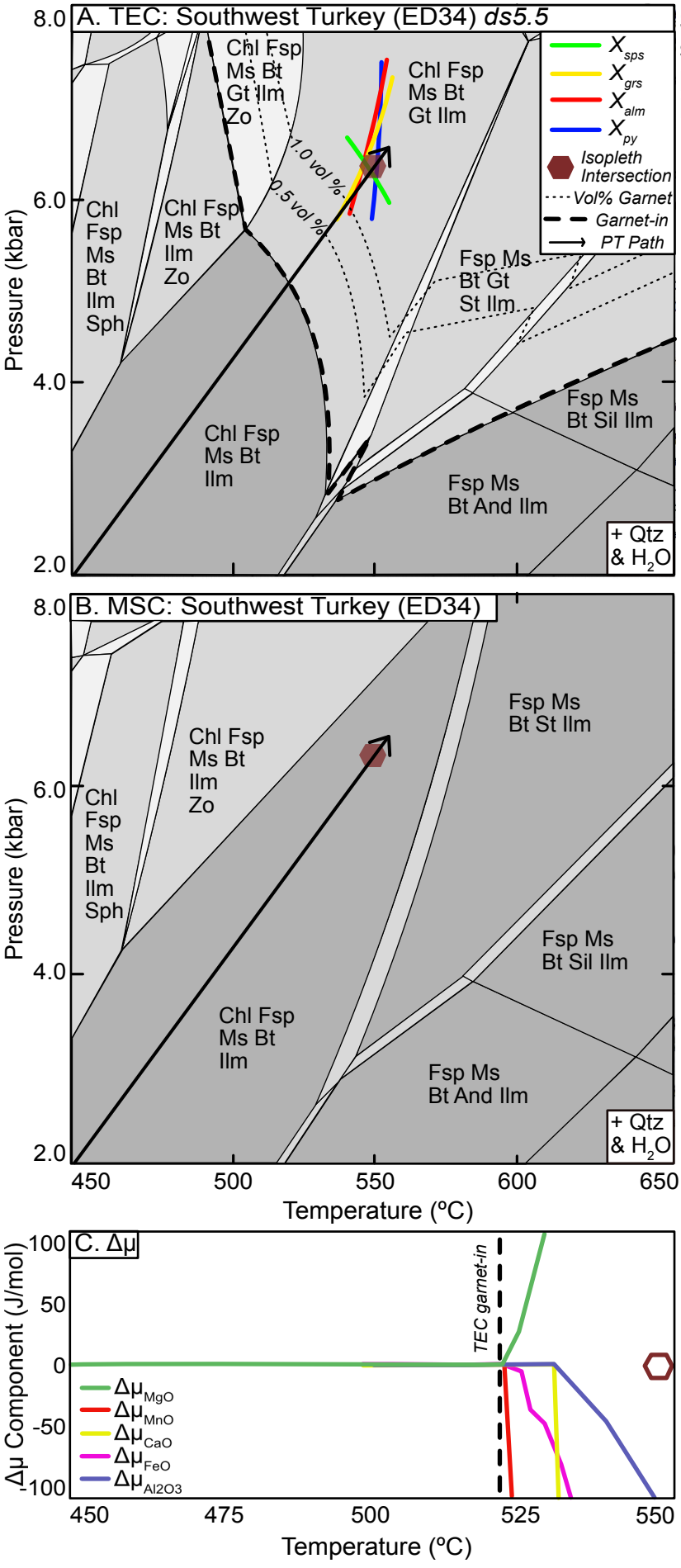

Supplemental Figure 4: A. TEC pseudosection for sample ED34 (Southwest Turkey). B. MSC pseudosection for sample ED34. C. $\Delta\mu_{component}$ along *P-T* path shown in A & B.

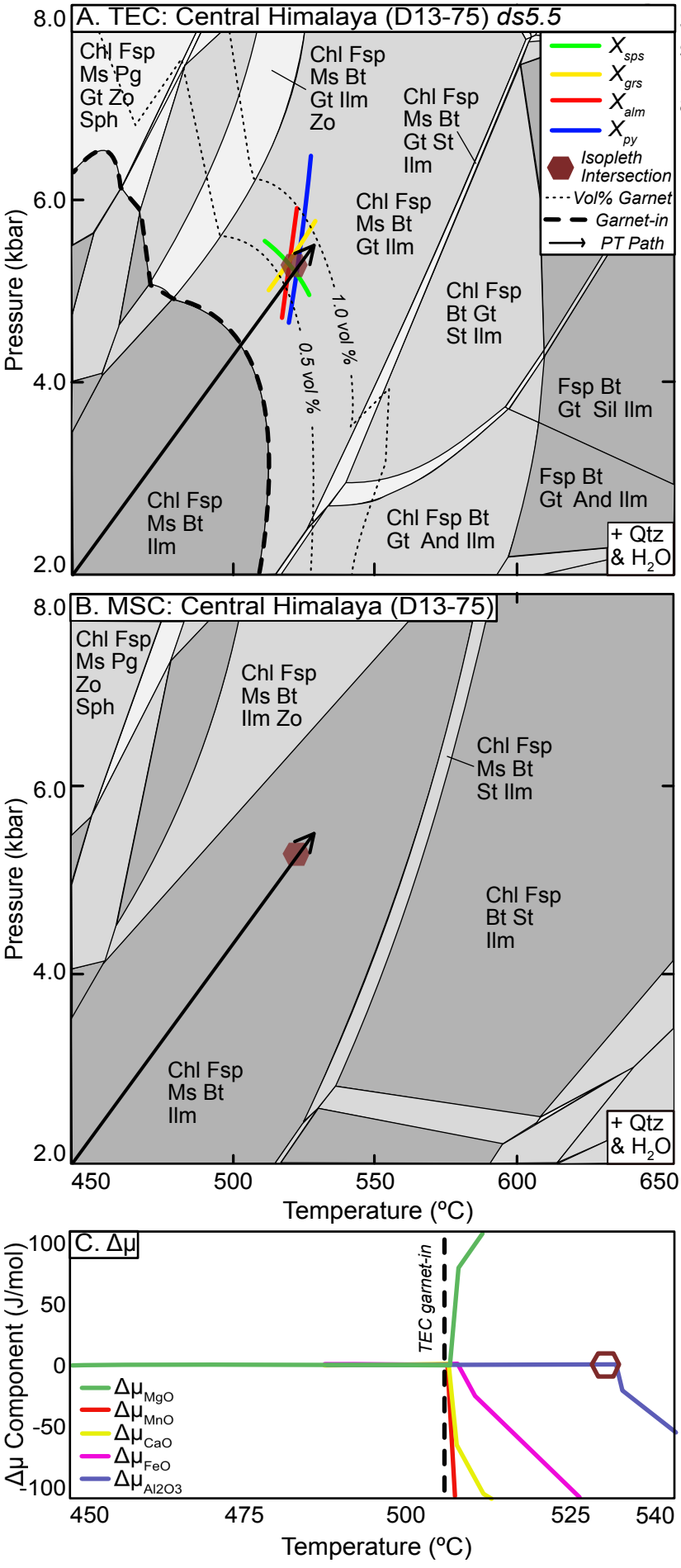

Supplemental Figure 5: A. TEC pseudosection for sample D13-75 (Central Himalaya). B. MSC pseudosection for sample D13-75. C. $\Delta\mu_{component}$ along *P-T* path shown in A & B.

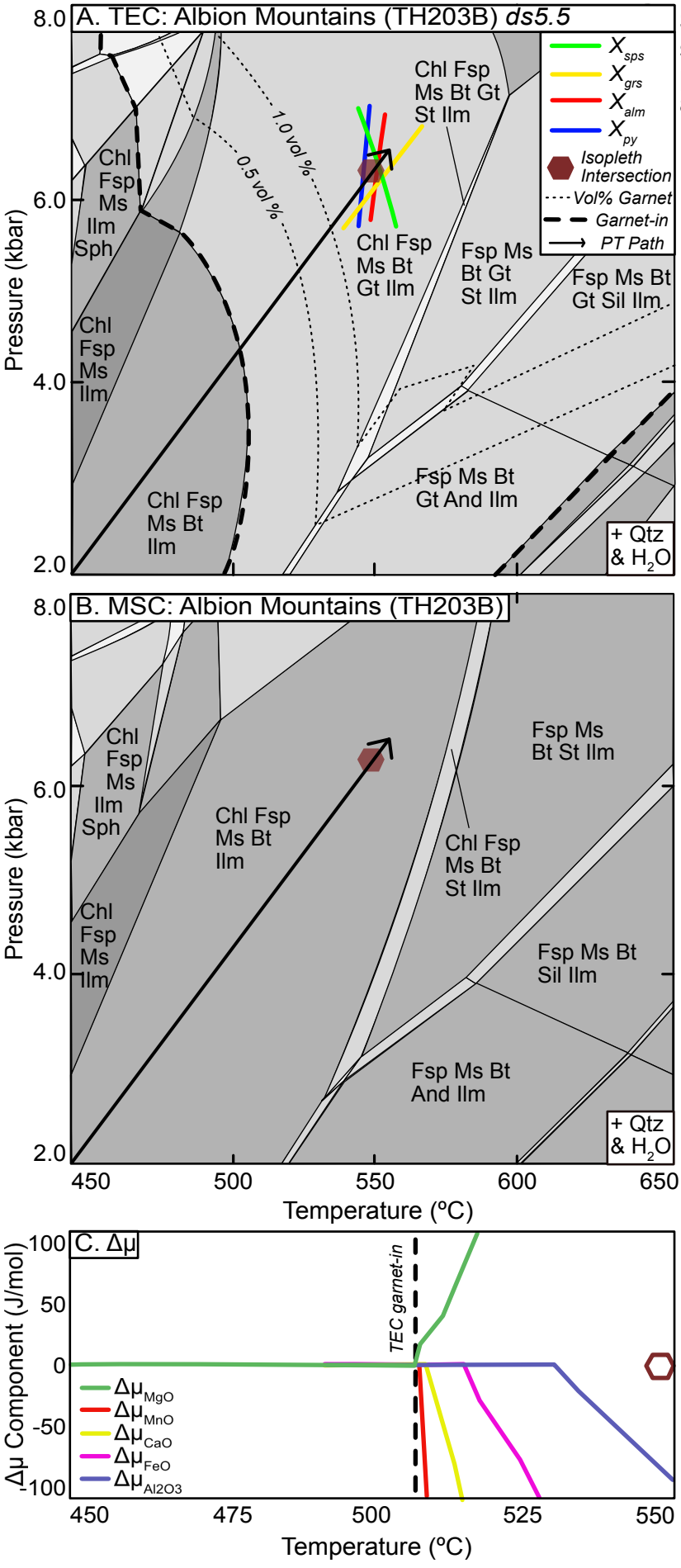

Supplemental Figure 6: A. TEC pseudosection for sample TH203B (Albion Mountains). B. MSC pseudosection for sample TH203B. C. $\Delta\mu_{component}$ along *P-T* path shown in A & B.

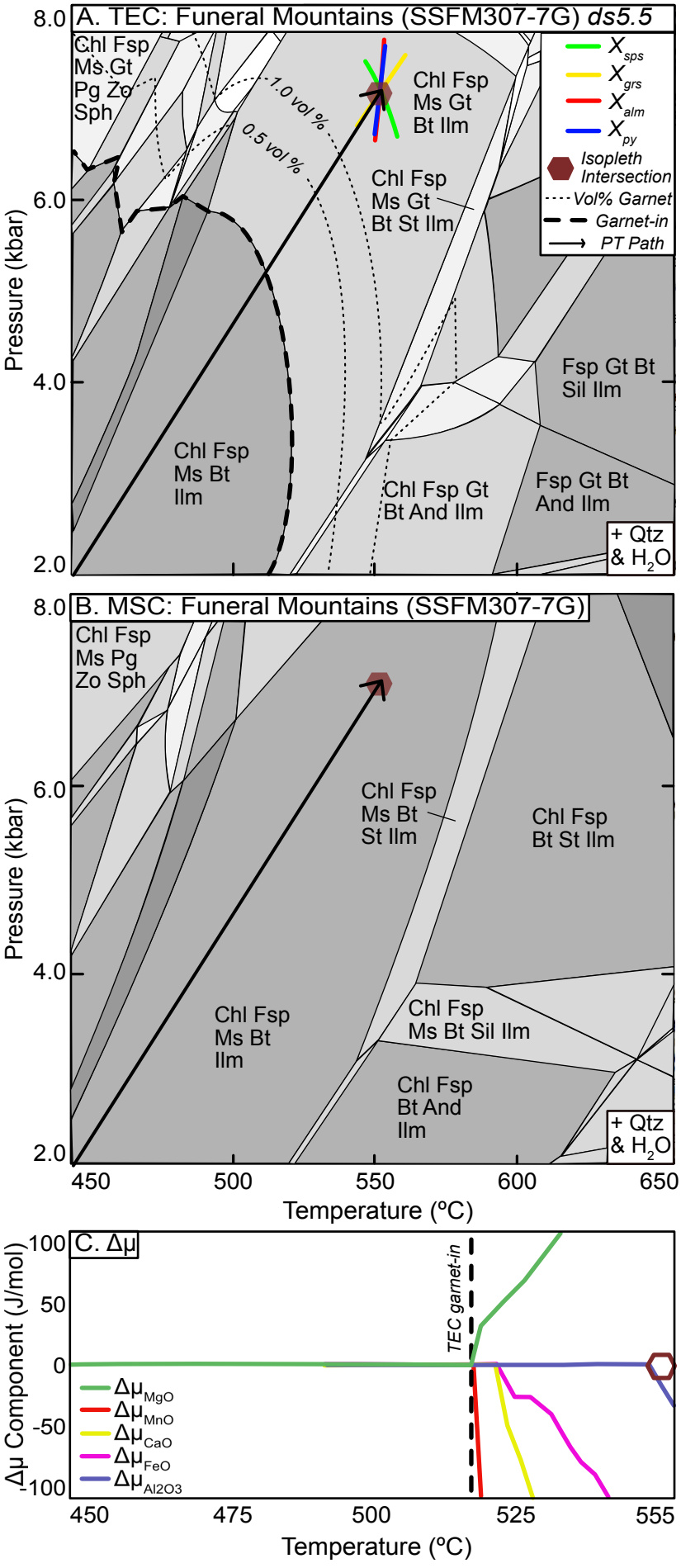

Supplemental Figure 7: A. TEC pseudosection for sample SSFM307-7G (Funeral Mountains). B. MSC pseudosection for sample SSFM307-7G. C. $\Delta\mu_{component}$ along *P-T* path shown in A & B.

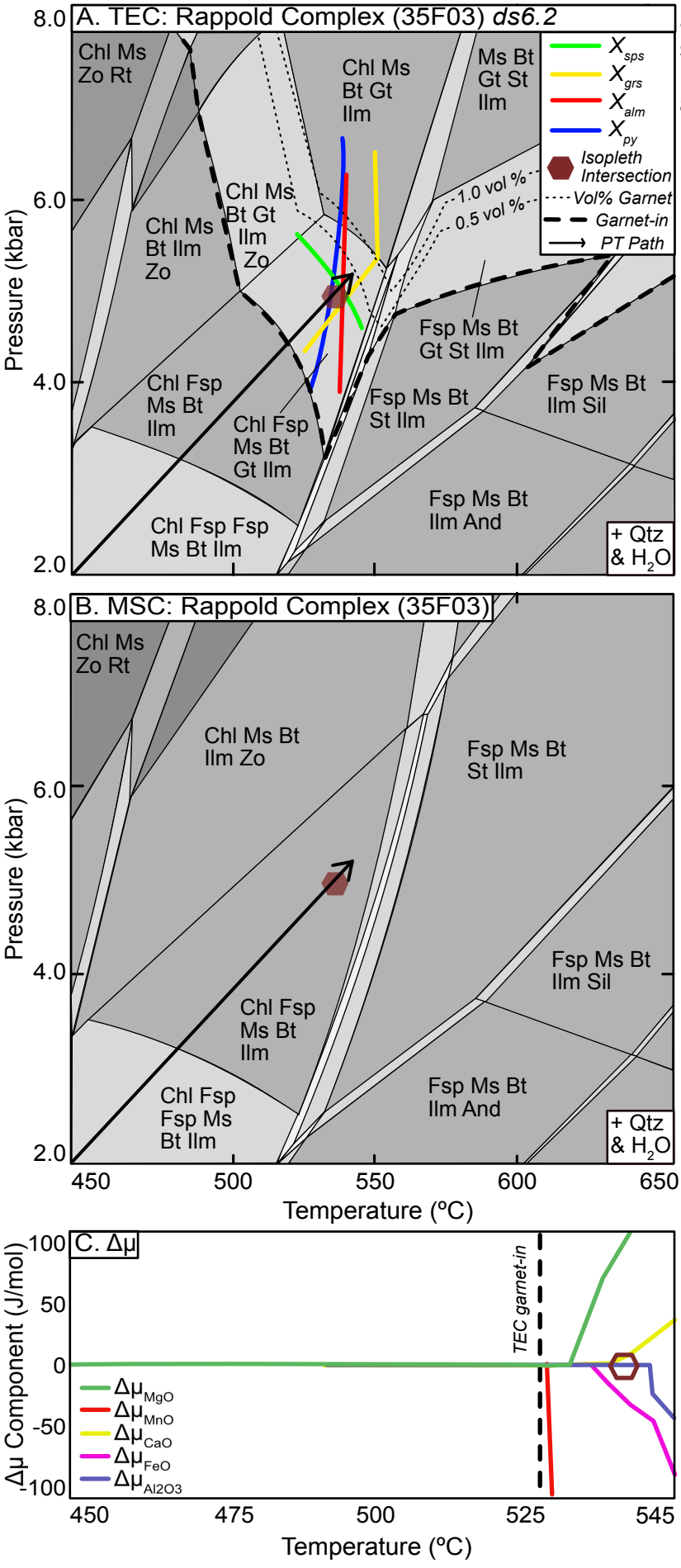

Supplemental Figure 8: A. TEC pseudosection for sample 35F03 (Rappold Complex) calculated with ds6.2 B. MSC pseudosection for sample 35F03. C. $\Delta\mu_{component}$ along *P-T* path shown in A & B.

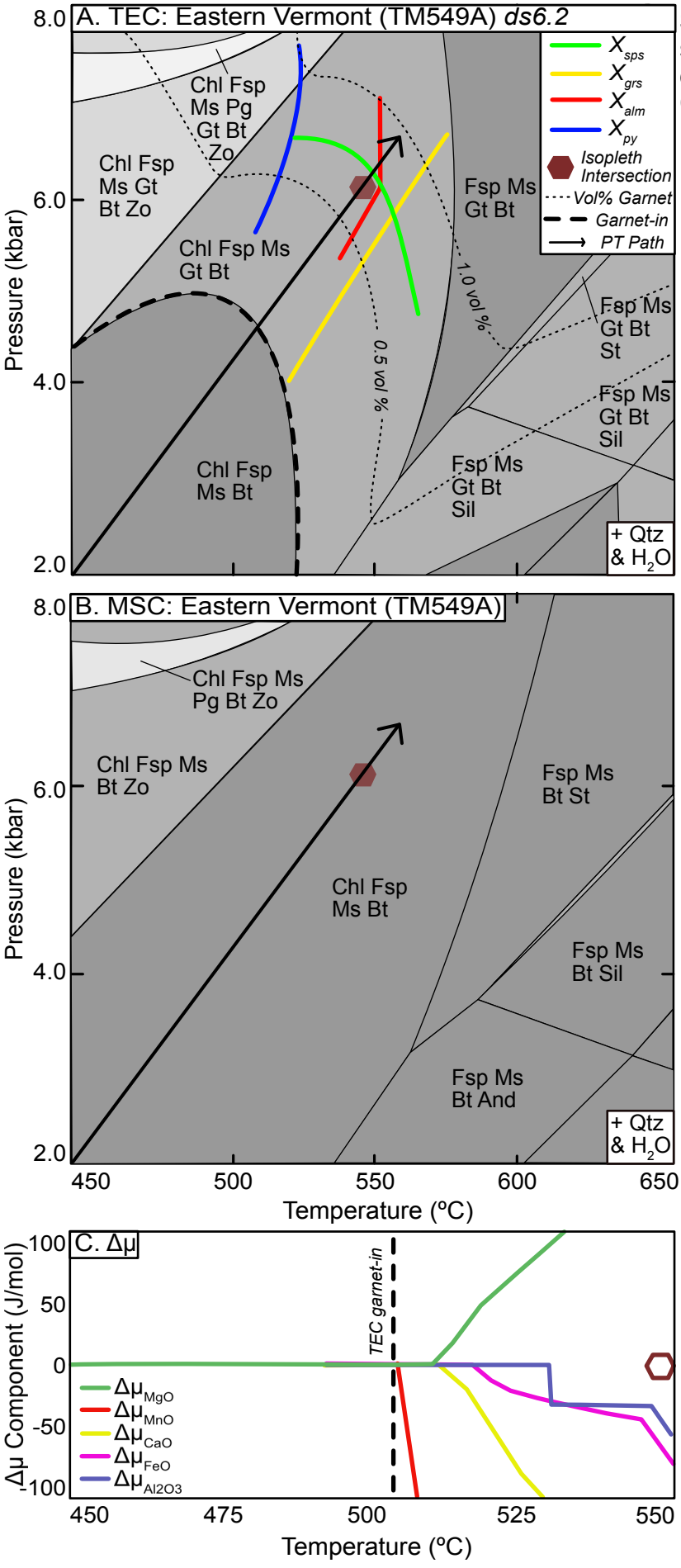

Supplemental Figure 9: A. TEC pseudosection for sample TM549A (Eastern Vermont) calculated with ds6.2. B. MSC pseudosection for sample TM549A. C. $\Delta\mu_{component}$ along *P-T* path shown in A & B.